

T-matching Networks for the Efficient Matching of Practical RFID Tags

J. Choo^{#1}, J. Ryoo^{#1}, J. Hong^{#1}, H. Jeon^{#1}, C. Choi^{#1} and Manos M. Tentzeris^{*2}

[#]*RFID Research Lab., LS Industrial Systems*

533 Hoge-dong, Dongan-gu, Anyang-si, Gyeonggi-do 431-080, Korea

¹*jychoo@lsls.biz*

^{*}*Georgia Electronic Design Center, School of Electrical and Computer Engineering,*

Georgia Institute of Technology, Atlanta, GA 30332-0250, USA

²*etentze@ece.gatech.edu*

Abstract— In this paper, we study T-matching networks that are commonly used for the efficient matching of UHF tags. In order to analyze relationship between T-matching geometry and antenna impedance, we interpret the transformer circuit as an equivalent circuit depending on the design parameters of the circuit. From the parametric study of the T-matching, we derive an optimized topology which is able to overcome electrically change of the geometry resulted from material loading. Next, based on the previous study, we design two types of tag antennas for practical item-level RFID applications that require the discrimination different objects. We calculate theoretically the minimum operating power of tags based on the computed antenna characteristics, antenna impedance, directivity, efficiency, regarding various dielectric constants. To verify the performance of the developed tags in practical conditions, we measure the minimum required power to activate tags on multiple objects in conjunction with commercial measurement system. As a result, the designed tags present almost consistent readability on materials from low to high dielectric constant. Thus, the results clearly verify that the appropriate T-matching geometry provides consistent readability in practical UHF RFID tags.

I. INTRODUCTION

In recent years, the interest in Radio Frequency Identification (RFID) systems has grown tremendously. Particularly, the passive ultra-high frequency (UHF) RFID systems are very attractive among the RFID systems using low frequency (LF, 125 KHz ~134 KHz), high frequency (HF, 13.56 MHz), ultra-high frequency (UHF, 860 MHz ~ 960 MHz), and microwave (2.4 GHz and 5.8 GHz) since they can provide superior reading range, fast reading speed and enhanced information storage ability. Furthermore, the low cost and power consumption of commercial UHF tag chips extend the applicability of UHF tags to item-level RFID's that require excellent readability on various objects.

In practical item-level RFID application, the readability of RFID system is strongly dependent on the performance of reader and tag antennas. Especially, the tag antenna design is the crucial factor for the item-level applications where the sensitivity of the tag performance on material properties mainly decides the identifying capability of the whole RFID system. Thus, In order to attain reliable readability regardless of objects, a lot of antenna structures were studied for the item-level RFID applications [1-3]. However most

investigated antennas were realized in rigid configurations with underlying grounds that limit their applicability in soft objects such as water and clothes. As an alternative approach, one novel antenna was proposed in [4] for better readability regardless of objects. In [4], the proposed antenna employs the T-matching network, which is composed of a dipole with a capacitive end-load and a T-matching structure of thick stripline, resulting in steady tag sensitivity (; minimum operating power) no matter what the dielectric properties of the mounted material are. As a result, it clearly points out that the antenna with the optimal T-matching networks can overcome electrical modification due to effective wave-length change when tags are mounted on many types of material objects.

In this paper, we firstly analysed the operating principle of a tag with T-matching network and verified that what T-matching geometry can invoke the constant readability. Next, to demonstrate our studied results, we designed tags with the optimal T-matching configuration and revealed that the newly developed tags have superior stable readability to the commercial tags through tag sensitivity measurement.

II. INTERPRETATION OF T-MATCHING NETWORK

The dipole (ground-backed monopole) antenna is a very popular antenna in various wireless applications because of its omni-directional radiation pattern, its simple structure, easy control of antenna impedance, the quality factor (Q) and its relatively small size. Especially, in RFID application, planar stripline and microstrip dipoles are commonly used as tag antennas. Also, to match practical capacitive RFID chips, people utilize inductively coupling feed [5], capacitively coupled structure [6], single and double T-matching [7, 8]. In this section, we examined the operation principle of tag dipoles with T-matching networks using equivalent circuit approach. Without loss of generality, to facilitate the analysis, we assume that the dipole-enabled tag is placed on 'air-like' substrate and objects. In the end, we introduce novel T-matching topologies that enable efficient matching regardless of material objects

A. Dipole Tag Antenna

Until now, a lot of researchers have modified the conventional dipole antenna topology using numerous

techniques to enhance its performance characteristics, such as bandwidth, efficiency, directivity and small size. For example, thick dielectric substrate and capacitive loading enable both bandwidth enhancement and size reduction since the added capacitance compensates the high inductance of the dipole, thus resulting in the decrease of the operating frequency and the increase of the quality factor [9]. Practically, many commercial tags hire a wide strip line as antenna body and a spacious loading bar to achieve broad bandwidth. Therefore we also engaged a thick planar dipole with the size of $0.5\lambda \times 0.2\lambda$ and the simulated impedance of $105+j14$.

B. Tag with T-matching Structure

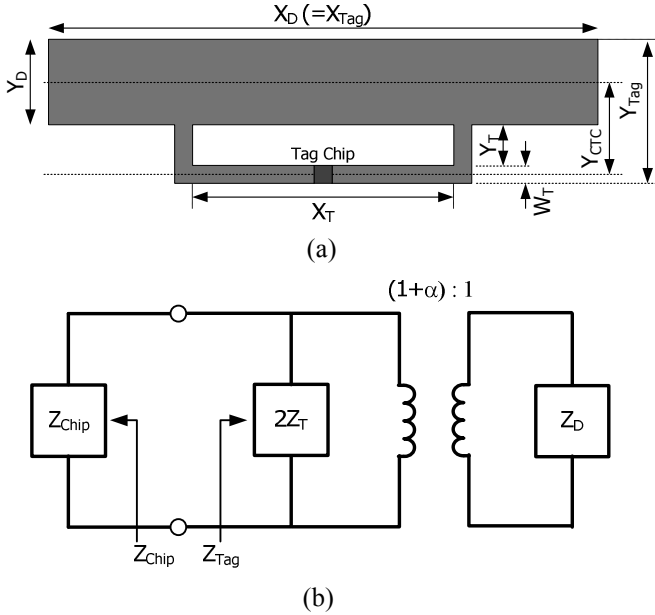


Figure 1 Dipole tag with T-matching structure; (a) Configuration of the tag. (b) Equivalent circuit model.

Fig. 1 shows the configuration and the equivalent circuit of a typical dipole tag with a T-matching geometry. As shown in Fig. 1(a), the planar tag is composed of a dipole, a T-matching stripline and a tag chip. We assumed that the tag is placed on the air substrate and object in order to apparently comprehend the operating principle regardless of the material effect. As a benchmarking tag chip, we used measured results of a commercial tag chip [10] with minimum operating power ($P_{Chipmin.}$) of -15 dBm and input impedance (Z_{Chip}) of $15-j180$ at 912 MHz that is operating frequency of UHF band RFID in South Korea. As shown in Fig. 1(b), the proposed T-matching circuit acts as transformer that matches the antenna impedance to the chip impedance through the adjustment of a new degree of freedom, the parameter α . To be specific, the parameters in Fig 1 are set as follows:

- Tag size : $X_{Tag} \times Y_{Tag}$
- Dipole size : $X_D \times Y_D = 0.5\lambda \times 0.2\lambda$
- T-matching size : $X_T \times Y_T$
- T-matching line width : W_T

- Y_{CTC} : Distance between central lines of dipole and T-matching line.
- Z_T : Impedance of shorted-circuit stub formed by the T-matching stripline and the dipole stripline .
- Z_D : Dipole impedance = $105+j14$
- Z_{Chip} : Chip impedance
- K : Wave number

$$P_{Chip} = P_{Ant}(1 - |\eta_{tag}|^2) = P_{Ant} \left(1 - \left| \frac{Z_{Ant} - Z_{Chip}^*}{Z_{Ant} + Z_{Chip}} \right|^2 \right) \quad (1)$$

$$Z_{Ant} = Z_{Chip}^* = \frac{2Z_T[(1+\alpha)^2 Z_D]}{2Z_T + (1+\alpha)^2 Z_D} \quad (2)$$

Also parameter α and Z_T in eq. (1) and (2) are defined as [9, 11]

$$\alpha = \frac{\log_e \left(\frac{Y_{CTC}}{W_T'} \right)}{\log_e \left(\frac{Y_{CTC}}{Y_D'} \right)} \quad \text{where } W_T' = 0.25W_T \text{ and } Y_D' = 0.25Y_D$$

$$Z_T = jZ_0 \tan \left(\frac{kX_L}{2} \right) \quad \text{where } Z_0 = 276 \log_{10} \left(\frac{Y_{CTC}}{\sqrt{W_T' Y_D'}} \right)$$

$$X_T = \frac{2}{k} \arctan \left[\left(\frac{(1+\alpha)^2 Z_D}{2(1+\alpha)^2 Z_D - 2} \right) \frac{1}{jZ_0} \right] \quad (3)$$

$$= \frac{2}{k} \arctan \left[\left(\frac{(1+\alpha)^2 Z_D}{Z_{Chip}^*} \right) \frac{1}{jZ_0} \right]$$

To investigate T-matching characteristics, we examine the relation between the antenna impedance and the T-matching geometry to maximize the power transfer from the antenna to the chip, or equivalently, the ratio of the delivered power to the chip (P_{Chip}) calculated from return loss (η_{Tag}) between the tag antenna and the chip as Eq. (1) [9]. Thus, the tag antenna should have the conjugate value of the chip impedance to enable the maximum transmitted power operation, as shown in Eq. (2) [9, 11]. Then utilizing Eq. (3), we can calculate the horizontal T-matching section size X_T as a function of the determined parameters α and Z_D .

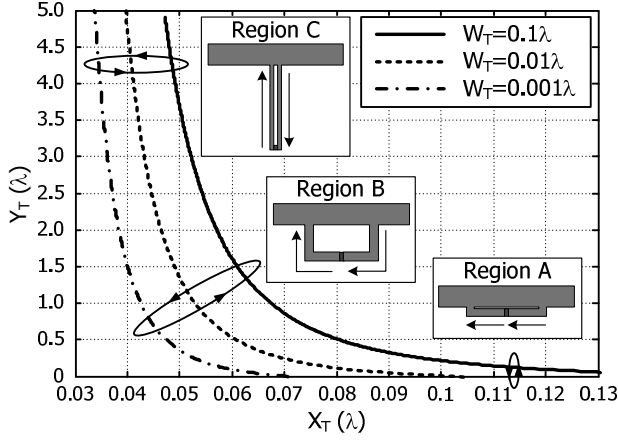


Figure 2 Geometry characteristic of T-matching for perfect conjugate matching with the chip.

Using Eq. (3) we can induce relation between X_T and Y_T for perfect conjugate matching with tag chip as shown in Fig. 2 that demonstrates the sensitivity of Y_T on X_T and W_T . To understand the results, we classified the results into three types of regions, which are region A, B and C, and approximately depict the antenna structure of the three groups with the main current flow on a T-matching stripline. Considering current distribution, material loading to tags in region A, B and C effectively affects significantly horizontal, both horizontal and vertical and vertical electrical length of T-matching structure respectively.

In detail, tags in region A are virtually insensitive on horizontal change of electrical length X_T since they feature nearly constant Y_T over a wide range of X_T . Therefore these tags are appropriate for practical applications on diverse materials. In contrast with the tags in region A, the tags in region B are greatly influenced by horizontal and vertical change of electrical length of X_T and Y_T . Thus they are applicable to only uniform material objects. In case of tags in region C, they have relatively stable characteristics in terms of Y_T . However they have the disadvantage of a too large vertical antenna size for practical item-level applications and high sensitivity of the antenna impedance on variation of W_T . As a conclusion, we confirmed that the T-matching configuration of region A is the optimum for tags requiring consistent readability in real-world RFID applications with numerous nonuniform dielectrics

III. TAG ANTENNAS FOR PRACTICAL ITEM-LEVEL APPLICATIONS

Here, we demonstrate validation of our research results by fabricating prototype tags and measuring the performances. The goal of the antenna design is to develop the tag to be able to apply to item-level RFID application with diverse material object. We designed a lot of tag antennas in Region A, considering return loss, radiating efficiency directivity in condition of attachment on object with $\tan\delta=0$, thickness=5mm. To prove the simulation results, the fabricated tags were measured regarding the tag sensitivity on

numerous real objects. The measured tag sensitivity is expressed comparing with a commercial tag. The measured results clearly show a good agreement with the simulated readable characteristics.

A. Antenna Designs and Characteristics

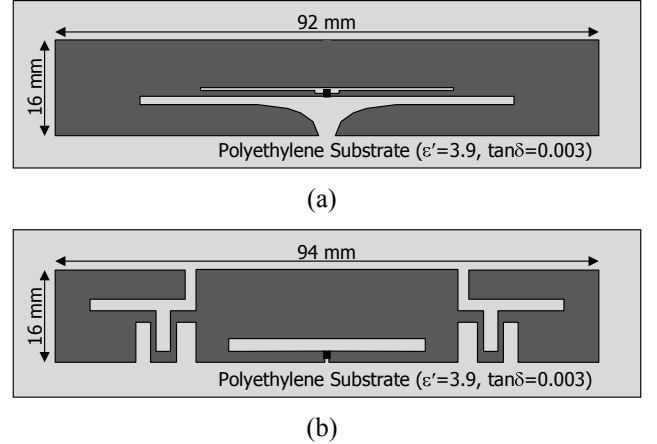


Figure 3 The optimized tags; (a) XCODE T tag with 92mm by 16mm, (b) XCODE Crab tag with 94mm by 16mm

$$P_{tag\ min.} = \frac{P_{chip\ min}}{(1-\eta_{tag}^2)Eff_{tag}D_{tag}} \quad (4)$$

$$= \frac{P_{min}(1-\eta_{reader}^2)Eff_{reader}D_{reader}}{\left(R_{fixed} \frac{4\pi}{\lambda}\right)^2} \quad (5)$$

Based on previous research, we designed two kinds of antennas, called as XCODE T tag and XCODE Crab tag, having stable readability regardless of materials as presented in Fig. 3. The tag antennas are printed strip line on polyethylene (PET, $\epsilon_r=3.9$, $\tan\delta=0.003$ and Thickness=50 μm) as a flexible substrate and designed to match to a measured chip impedance $Z_{chip}=15-j180\ \Omega$ at 912 MHz. In antenna design process, we significantly considered tag sensitivity ($P_{Tagmin.}$) corresponding to change of the material that tags are mounted on. To be specific, we derived the tag sensitivity as function of dielectric constant of object ($\tan\delta=0$, Thickness=5mm) using Eq. (4), where return loss (η), radiation efficiency (Eff) and directivity (D) are computed using a commercial electromagnetic field simulator of IE3D of Zeland [9, 12].

Fig. 4 shows the computed tag sensitivity at 912 MHz as a function of dielectric constant in comparison with a well-known commercial tag, the Alien Technology Squiggle tag [14]. For more quantitative analysis, we defined material bandwidth as

$$\text{Material bandwidth (MB)} = \text{Maximum } \epsilon_r - \text{Minimum } \epsilon_r$$

where *Maximum ϵ_r* and *Minimum ϵ_r* means maximum and minimum dielectric constants to have a higher sensitivity of 3 dB than the lowest sensitivity. Also, Table I represents

summary of computed results regarding information of tag chip, tag size and material bandwidth

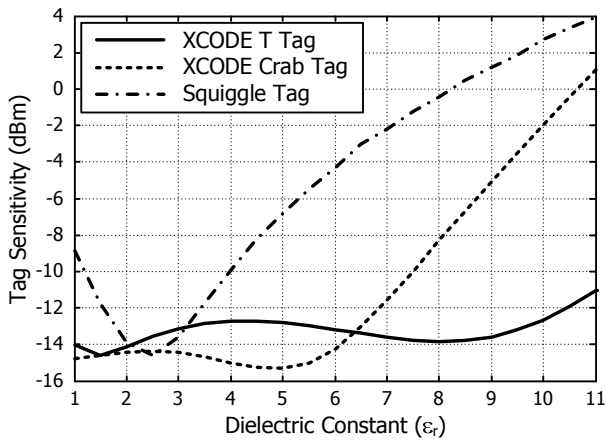


Figure 4 Calculated tag sensitivity

TABLE I
SIMULATED RESULTS

	XCODE T tag	XCODE Crab tag	Alien Squiggle tag
Tag Chip	Monza 3 [10]		Higgs 2 [13]
Mea. Z_{Chip} at 912 MHz	15-j180 Ω		9-j110 Ω
$P_{Chipmin.}$	-15 dBm		-14 dBm
Tag Size	92 mm \times 16 mm	94 mm \times 16 mm	97 mm \times 11 mm
Min. Tag Sensitivity	-15.4 dBm ($\epsilon_r=4.9$)	-14.7 dBm ($\epsilon_r=1.5$)	-14.6 dBm ($\epsilon_r=2.5$)
Material Bandwidth	5.72 ($\epsilon_r:1.0 \sim 6.72$)	9.70 ($\epsilon_r:1.0 \sim 10.70$)	2.08 ($\epsilon_r:1.47 \sim 3.55$)

B. Experimental Results

TABLE II
MEASURED RESULTS

	Tag Sensitivity (dBm)				Dev. (dB)
	Foam (T=5)	Wood (T=8.4)	FR4 (T=5)	Glass (T=4.8)	
XCODE T tag	-13.79	-15.42	-15.72	-13.87	1.93
XCODE Crab tag	-15.82	-15.25	-15.26	-15.75	0.57
Alien Squiggle tag	-12.70	-13.64	-14.91	-14.86	2.21

To verify the simulation results, we measured the tag sensitivity of fabricated tags and Squiggle tag on various materials in an anechoic chamber excluding environmental electro-magnetic interference. Besides we utilized a commercial measurement system, Tagformance Lite of Voyantic Corporation [15], which basically calculates the tag sensitivity using Eq. (5). Table II presents the measured tag sensitivity when the tags are mounted on foam (Thickness=5

mm), wood (Thickness=8.4 mm), FR4 (Thickness=5 mm) and glass (Thickness=4.8 mm). Considering deviation of the measured tag sensitivity, the developed tags have superior stable detectable characteristic to a commercial tag in condition of the proposed objects. Especially XCODE Crab tag is a remarkable stable performance with deviation of only 0.57 dB on every real object. Also we think a little disagreement of simulated and measured results would come from diverse the size and thickness of underlying material differed from infinite size and constant thickness of 5mm in simulation.

IV. CONCLUSIONS

In this paper, we investigated the fundamental properties of the printed T-matching circuits to enable more robust tag for item-level RFID applications. Firstly, we examined the effect of the T-matching geometry on whole antenna impedance using equivalent circuit. We confirmed that T-matching structure enhances the robustness of the tags to detuning effects from material loading. Secondly, to demonstrate the research results, we developed two tags with the adequate T-matching and calculated tag sensitivity as a function of dielectric constant where tag attached on diverse materials. Additionally, through the measurement of the designed tags, we also confirmed almost constant readability, which shows good agreement with the computed results.

REFERENCES

- [1] W. Choi, J. Kim, J. H. Bae and G. Choi, "A small RFID tag antenna using proximity-coupling to identify metallic objects," *Microwave and Optical Technology Lett.*, vol. 50, pp. 2978-2981, Nov. 2008
- [2] Son, H.-W., "Design of RFID tag antenna for metallic surfaces using lossy substrate," *Electron. Lett.*, vol. 44, pp. 711-713, June. 2008.
- [3] S. L. Chen and K. H. Lin, "A Slim RFID Tag Antenna Design for Metallic Object Applications," *IEEE Antennas and Wireless Propagat. Lett.*, vol. 7, pp. 729-732, Jan. 2009
- [4] J. Choo, J. Ryoo and J. Hong, "Novel RFID Tag Antenna with Stability to Material," *IEEE Antennas and Propagation Society International Symp.*, pp. 1-4, July 2008.
- [5] C. Choo and H. Ling, "Design of electrically small planar antennas using inductively coupled feed," *Electron. Lett.*, vol. 39, pp. 1563-1565, Oct. 2003
- [6] C. C. Chang and Y. C. Lo, "Broadband RFID tag antenna with capacitively coupled structure," *Electron. Lett.*, vol. 42, pp. 1322-1323, Nov. 2006
- [7] C. Cho, H. Choo and I. Park, "Design of planar RFID tag antenna for metallic objects," *Electron. Lett.*, vol. 44, pp. 175-177, Jan. 2008
- [8] C. Cho, H. Choo and I. Park, "Broadband RFID tag antenna with quasi-isotropic radiation pattern," *Electron. Lett.*, vol. 41, pp. 1091-1092, Sept. 2005
- [9] C. A. Balanis, *Antenna theory analysis and design*, New York: John Wiley & Sons, 1997.
- [10] Impinj Monza 3 Datasheet. Online: www.impinj.com/products/tag-chips.aspx
- [11] G. Marrocco, "The art of UHF RFID antenna design: impedance-matching and size-reduction techniques," *IEEE Antennas Propagat. Mag.*, vol. 50, pp. 66-79, Feb. 2008
- [12] IE3D 14.1. Online: www.zeland.com
- [13] Alien Higgs 2 Datasheet. Online: www.alientechnology.com/docs/products/DS_H2.pdf
- [14] Alien ALN-9540 Product Datasheet. Online: www.alientechnology.com/docs/products/DS_ALN_9540_Squiggle.pdf
- [15] Tagformance Lite. Online: www.voyantic.com